Assessing water erosion processes in degraded area using unmanned aerial vehicle imagery

Paulo Siqueira Junior, Marx Leandro Naves Silva, Bernardo Moreira Cândido, Fabio Arnaldo Pomar Avalos, Pedro Velloso Gomes Batista, Nilton Curi, Wellington de Lima, John Norman Quinton

Assessing Water Erosion Processes in Degraded Area Using Unmanned Aerial Vehicle Imagery

Paulo Siqueira Junior[(1)] (iD)**, Marx Leandro Naves Silva**[(2)*] (iD)**, Bernardo Moreira Cândido**[(3)] (iD)**, Fabio Arnaldo Pomar Avalos**[(1)] (iD)**, Pedro Velloso Gomes Batista**[(1)] (iD)**, Nilton Curi**[(1)] (iD)**, Wellington de Lima**[(1)] (iD) **and John Norman Quinton**[(2)] (iD)

[(1)] Universidade Federal de Lavras, Departamento de Ciência do Solo, Lavras, Minas Gerais, Brasil.
[(2)] Lancaster University, Lancaster Environment Centre, Lancaster, Lancashire, United Kingdom.
[(3)] Instituto Agronômico de Campinas, Centro de Solos e Recursos Ambientais, Campinas, São Paulo, Brasil.

ABSTRACT: The use of Unmanned Aerial Vehicles (UAVs) and Structure from Motion (SfM) techniques can contribute to increase the accessibility, accuracy, and resolution of Digital Elevation Models (DEMs) used for soil erosion monitoring. This study aimed to evaluate the use of four DEMs obtained over a year to monitor erosion processes in an erosion-degraded area, with occurrence of rill and gully erosions, and its correlation with accumulated rainfall during the studied period. The DEMs of Geomorphic Change Detection (GCD) of horizontal and vertical resolutions of 0.10 and 0.06 m were obtained. It was possible to detect events of erosion and deposition volumes of the order of 2 m^3, with a volumetric error of ~50 %, in rills and gullies in the initial stage denominated R and GS-I, respectively. Events of the order of 100 m^3, with a volumetric error around 14 % were found for advanced gullies, a segment denominated GS-II. In the three studied erosion situations, the deposition volume increased with the accumulated rainfall. The segments R and GS-I presented an inverse relationship between erosion volume and accumulated rainfall during the studied period. This behaviour can be explained by the dynamics of the deposition and erosion volumes during the erosion process. In the GS-II segment, erosion and deposition volumes were proportional and a direct relation with the cumulative rainfall over the studied period and a low percentage of volumetric error were found.

Keywords: Gully, UAV, digital elevation model, structure-from-motion.

INTRODUCTION

Rills and gullies are occurring features in hillslopes. Rills formation is predominantly driven by concentrated surface flow, while gullies, besides surface flow, may also initiate from subsurface flow and other environmental factors, such as climate, soil, and vegetation cover. Both processes cause significant amounts of soil loss and sediment production (Poesen et al., 2003; Gao, 2013).

The dynamics of this processes can be studied at different scales and with different objectives, ranging from inventory mapping on a regional scale to assessing the expansion of gullies with a greater level of detail (Betts et al., 2003; Di Stefano et al., 2017). A wide variety of measuring techniques and equipment can be used. The traditional techniques include different devices, such as graduated stakes, measuring tapes, topographic profilers, and total station to survey cross sections for volume determinations (Casalí et al., 2006; Ehiorobo and Audu, 2012; Gómez-Gutiérrez et al., 2012). These techniques, although providing satisfactory approximations for erosion monitoring studies in two-dimensional evaluations, demand a great amount of time and can present significant errors in volumetric calculations (Castillo et al., 2012).

In contrast, the use of high resolution Digital Elevation Models (DEMs) has been recognized as an useful tool for measuring land surface change processes (Tarolli, 2014; Passalacqua et al., 2015), since it allows the detection of geomorphic changes by means of Geomorphic Change Detection (GCD) analysis for measuring erosion and deposition volumes (Wheaton et al., 2010). Moreover, topographic attributes related to these erosion processes, such as slope, exposure, curvature, and direction of preferential water flow can be assessed (Ouédraogo et al., 2014).

In this context, the use of Unmanned Aerial Vehicles(UAVs) and Structure from Motion (SfM) photogrammetry techniques can contribute significantly to the increase of accessibility, performance, and accuracy in the acquisition of DEM and high orthoimage resolutions and accuracy for monitoring erosion processes (Castillo et al., 2012; D'Oleire-Oltmanns et al., 2012; Stöcker et al., 2015; Wang et al., 2016; Glendell et al., 2017).

Therefore, this study aimed to evaluate the sensitivity of GCD analysis of a time series of DEMs obtained using UAV and photogrammetry using the SfM technique for the detection of erosion processes in gullies of two different stages of evolution and rills, in an area degraded by water erosion located in Itumirim, Minas Gerais State, Brazil.

MATERIALS AND METHODS

Study area

The study area has 0.83 ha, located in the municipality of Itumirim, state of Minas Gerais, Brazil (Figure 1). The municipality is located in the Campos das Vertentes physiographic zone, with rainy Cwa-temperate climate (cold and dry winter and hot and humid summer) (Dantas et al., 2007), according to Köppen classification system.

It is included in the Atlantic Plateau, specifically in the Upper Grande River, where the predominant relief is undulated. Geologically, the region is predominantly represented by gabbro and melanocratic gneiss.

The native vegetation is characterized by tropical semi-perennial forest. The predominant land uses are annual crops and planted pastures. The study area is heavily degraded by water erosion, with a high incidence of rill and gully erosions and it was used as a lending area for the recomposition of unpaved roads. The soil in the area is classified as a *Cambissolo Háplico* according to the Brazilian System of Soil
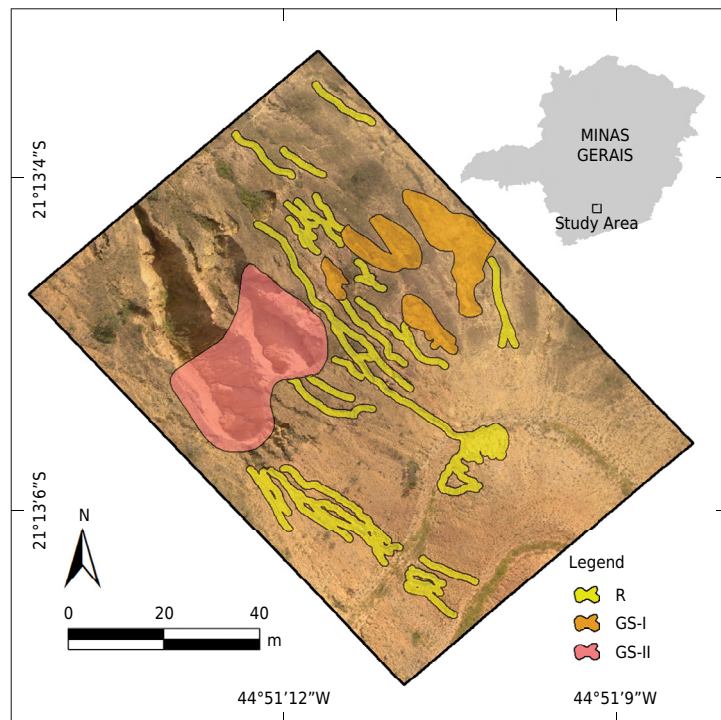
Figure 1. Location of the study area and the analysed segments in Itumirim, Minas Gerais, Brazil. R: deep rills; GS-I: small gullies; and GS-II: large gullies.

Classification (Santos et al., 2018) [Inceptisol (Soil Survey Staff, 2014) or Cambisol (IUSS Working Group WRB, 2015)].

MATERIALS AND METHODS

The GCD allows inferring erosion patterns based on the monitoring of topographic surfaces. To assess the sensitivity of GCD in a time series of DEMs obtained from UAV and SfM photogrammetry, the following sequence of activities was performed: (1) acquisition of multi-temporal DEM and orthoimages; (2) subdivision of the study area into two gully segments of different development stages and a segment of rills; (3) comparison between DEMs using GCD analysis; and (4) rainfall information from a climatological station near the study area and evaluation of the correlation between estimated erosion and deposition volumes with the accumulated rainfall during the studied period.

Multi-temporal series of digital elevation models and orthomosaic maps

To obtain the multi-temporal series of DEMs and orthoimages, the following steps were performed: (1) installation of 20 permanent ground control points throughout the studied area, made from 0.80 m long concrete landmarks and acrylic plates of 0.30 × 0.30 m; (2) georeferencing of the control points using a pair of Geodesic GNSS receivers in RTK mode (JAVAD, Triumph-1 model); (3) performing planned stand-by flights on the dates described in table 1, using the standard DJI Phanton-3 UAV and the Litchi application; (4) processing the images acquired in each flight, using the Agisoft Photoscan Professional® v1.4, being exported as GeoTIFFfiles. The information about the point cloud density, DEM, GSD, and alignment error are shown in table 2.

Accuracy of DEMs, derivation, and propagation of the altimetric error

The altimetric accuracy of DEMs was evaluated using seven of the 15 land control points as check points, thus obtaining the average altimetric error of the checkpoints for each DEM (Table 3). However, using only the accuracy obtained by the control points

to derive the altimetric error of DEMs can substantially underestimate the magnitude of the altimetric error. Thus, an error value of 6.3 cm was used for all DEMs, which was obtained through simulations performed prior to this study.

The attributed altimetric error propagation was obtained by the root of the sum of the squares of the individual altimetric errors of each DEM, as suggested by Wheaton et al. (2010). This calculation was performed using the Geomorphic Change Detection extension of the ArcGIS 10.3 software.

Subdivision of the study area

The study area was subdivided into two segments of gullies at different stages of evolution and a segment of rills in order to standardize the type and magnitude of the erosion processes to be monitored (Figure 1). The segment denominated GS-II (large gully erosion, gully stage II) has an area equivalent to 633 m^2 and represents

Table 1. Settings used in flight plans for aerial surveys on different dates

DEM	Date	Height	FS	LS	FO	LO	NDP	Area
		——— m ———			——— % ———			ha
DEM_1	May 20th, 2016							
DEM_2	August 18th, 2016	25	12	15	70	70	104	1.7
DEM_3	March 15th, 2017							
DEM_4	May 26th, 2017							

DEM: digital elevation model; FS: frontal spacing between images; LS: lateral spacing between images; FO: frontal overlap between images; LO: lateral overlap between images; NDP: number of digital photos.

Table 2. Geomorphic change detection points cloud density, error of image alignment accuracy, and spatial resolution of the digital elevation model

DEM	PCD	GCD		Error
		Minimum	Used	
	pt m^{-2}	——— cm pixel^{-1} ———		pixel
DEM_1	353	5.32	10	0.673
DEM_2	384	5.10	10	0.694
DEM_3	216	6.80	10	0.947
DEM_4	306	5.72	10	0.852

DEM: Digital Elevation Model; PCD: Point Cloud Density; GCD: Geomorphic Change Detection; Error: image alignment error.

Table 3. Altimetric error obtained by the checkpoints and altimetric error attributed to DEMs

DEM	Error Z	
	Checking	Assigned
	——— cm ———	
DEM_1	0.650	6.300
DEM_2	0.045	6.300
DEM_3	1.600	6.300
DEM_4	1.080	6.300
DEM_5	2.070	6.300
DEM_6	1.480	6.300

DEM: digital elevation model.

gullies of width between 10 to 15 m and depths ranging from 5 to 15 m; the segment denominated GS-I (small gully erosion, gully stage I) has an area equivalent to 390 m² and represents gullies ranging from 2 to 5 m wide and 2 to 4 m deep; and the segment denominated R (rill erosion) has an area equivalent to 823 m² and represents rills of 0.5 to 2 m wide and up to 1 m deep. The segments were manually delineated using ancillary information from DEMs and the orthoimages. It was sought to delimit the segments in areas without the presence of vegetation or excessive shading that could add errors in the GCD analyses.

Geomorphic changes detection analysis

The GCD analyses were performed by comparing DEM_1 with the other consecutive DEMs (Table 4). The GCD analyses followed the following workflow: (1) DEMs import (Add DEM survey); (2) insertion of the uniform altimetric error of each DEM (Derive Error Surface: uniform width: 6.3 cm); (3) GCD analysis (add change detection) using the Uncertainty Analysis Method (Propagated Errors).

Correlation of the detected geomorphic changes with the accumulated rainfall

The rainfall data used in this study were obtained from a climatic station located 1 km from the study area. Figure 2 shows the monthly distribution of rainfall and the indication of the months in which the flights were performed. The cumulative rainfall values were computed for each date range between the acquisition of DEM_1 and each analysed DEM.

Table 4. Altimetric errors in the geomorphic change detection analysis

Analysis GCD	DEM		Altimetric error	
	Reference	Analized	Uniform	Propagation
			cm	
1		DEM_2		
2	DEM_1	DEM_3	6.3	8.9
3		DEM_4		

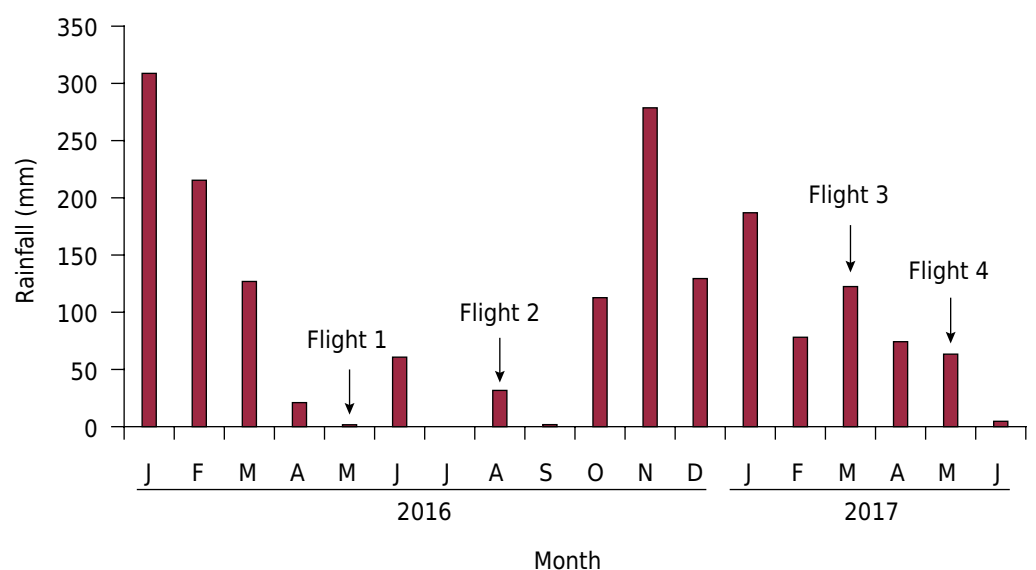GCD: Geomorphic Change Detection; DEM: digital elevation model.

Figure 2. Monthly distribution of rainfall indicating the months in which the flights were performed in the area degraded by water erosion.

RESULTS

Geomorphic Change Detection

The results of the GCD analysis in relation to DEM_1 and other DEM of the multi-temporal series are shown in table 6 and figure 3. Figure 3 indicates mass displacement (MD) and deposition (D) of the soil in the studied area.

The volumetric errors of the R and GS-I segments reached mean values of 58 and 46 %, respectively (Table 6). An abrupt rise in erosion and deposition values detected in GCD analysis between DEM_3 and DEM_1 was observed (Table 6), when compared to GCD analysis values of DEM_2 with DEM_1.

Segment GS-II presented lower values of volumetric error and a greater percentage of altered areas than segments R and GS-I.

Correlation of detected geomorphic changes and accumulated rainfall

The results of the correlation analysis between the erosion and deposition volumes with the accumulated rainfall in each period are shown in figure 4.

Table 5. Reference and analysis of DEM with their respective dates and rainfall data

RDEM		ADEM		CR
DEM	Date	DEM	Date	
				mm
DEM_1	May 20th, 2016	DEM_2	August 18th, 2016	65.4
DEM_2	August 08th, 2016	DEM_3	March 15th, 2017	875.6
DEM_3	March 15th, 2017	DEM_4	May 26th, 2017	191.2

RDEM: reference digital elevation model; DEM: digital elevation model; ADEM: analysis digital elevation model; CR: cumulative monthly rainfall.

Table 6. Geomorphic Change Detection analyses for the rill erosion (R), small gully erosion (GS-I) and large gully erosion (GS-II)

RDEM	ADEM	Area	EV	DV	VE
		%	m^3		%
	R				
	DEM _2	2.38	3.69	0.10	51.75
DEM_1	DEM _3	2.07	0.75	1.82	66.07
	DEM _4	1.60	0.37	1.97	56.32
	GS-I				
	DEM _2	7.92	6.60	0.37	43.92
DEM _1	DEM _3	13.10	2.28	8.38	47.56
	DEM _4	4.75	1.60	2.25	47.64
	GS-II				
	DEM _2	18.59	27.88	21.23	23.86
DEM _1	DEM _3	41.73	112.24	138.67	10.49
	DEM _4	32.86	141.85	106.03	8.36

RDEM: reference digital elevation model; ADEM: analysis digital elevation model; EV: erosion volume; DV: deposition volume; VE: volumetric error.
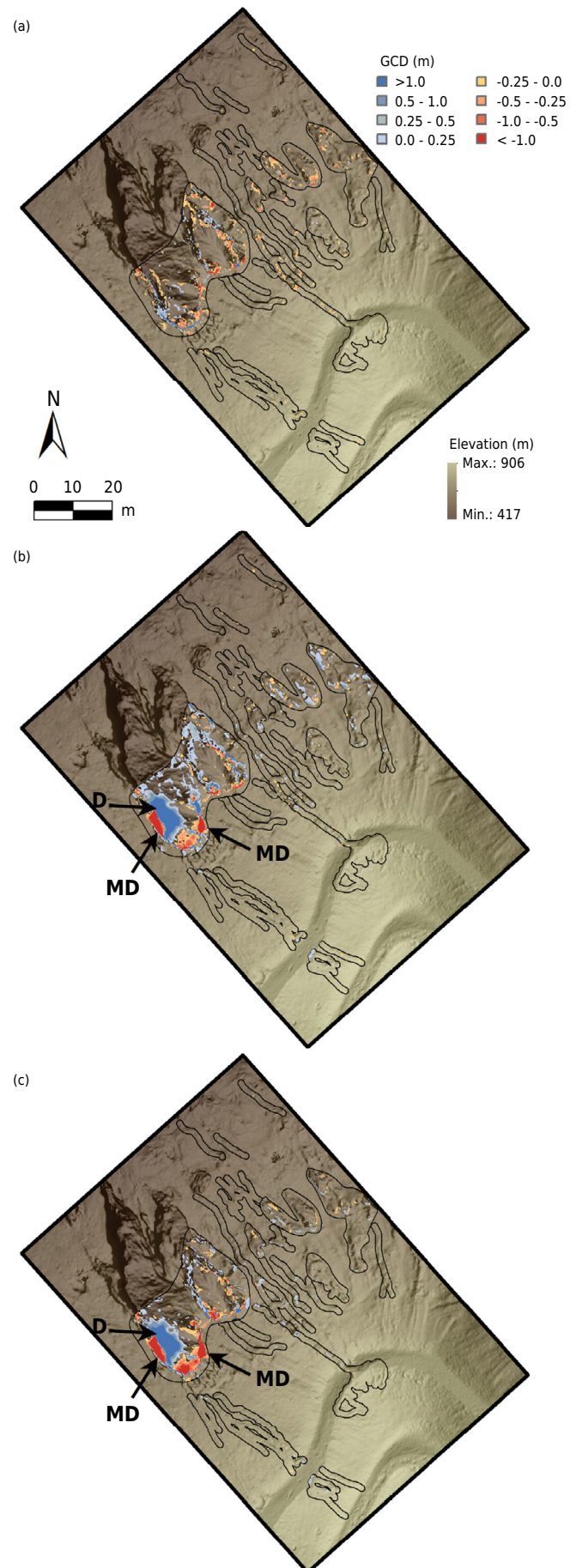
Figure 3. Geomorphic Change Detection analysis between DEM_1 and DEM_2 (a), DEM_1 and DEM_3 (b), and DEM_1 and DEM_4 (c). Arrows indicate mass displacement (MD, red areas) and deposition (D, blue areas).
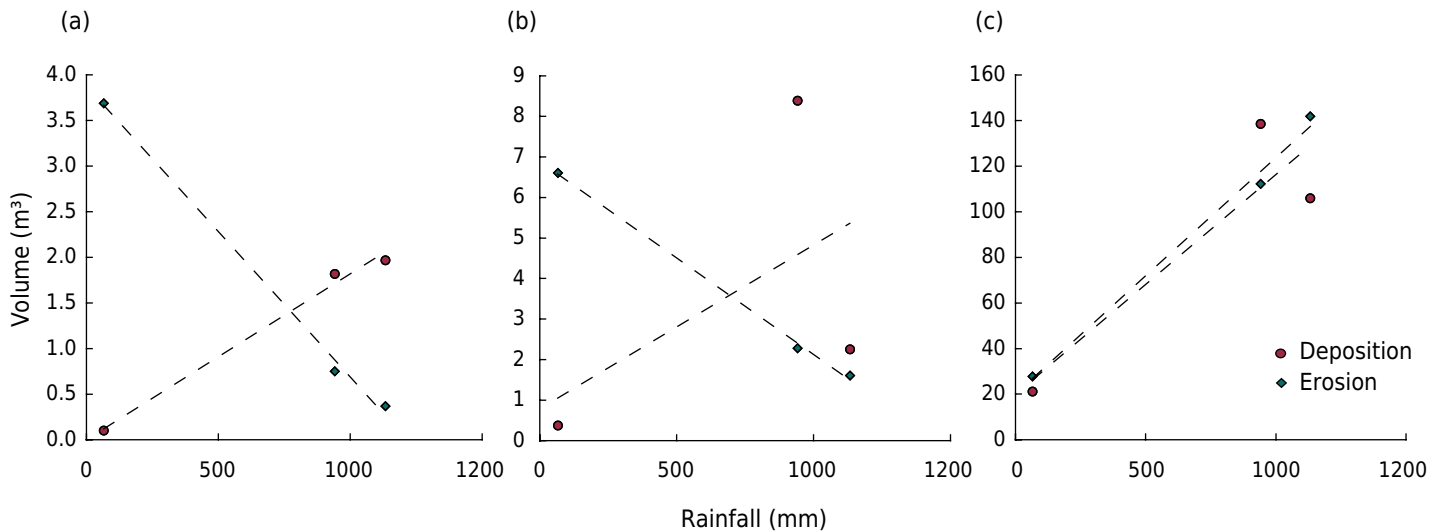
(a)

(b)

(c)

Figure 4. Correlation between erosion and deposition volume and accumulated rainfall. R: deep rills (a); GS-I: small gullies (b); and GS-II: large gullies (c).

As can be observed in figures 4a and 4b, the erosion values for segments R and GS-I presented an inverse relationship with the accumulated rainfall values. In contrast, segment GS-II presented a direct relationship between the erosion and deposition values and rainfall accumulation (Figure 4c), which is an expected behaviour of active gullies of this size.

As a result of this study, a series of four DEMs of GSD of 10 cm with altimetry precision in the order of centimetres were performed. In 13 months (May 2016 to May 2017), segment R (0.5 to 2 m wide and up to 1 m deeprills) presented a total erosion volume of 0.37 m^3 and a deposition of 1.97 m^3, and an average volumetric error of 58 %. As for segmentGS-I (2 to 5 m wide and 2 to 4 m deep gullies) presented total erosion volume of 1.6 m^3 and deposition of 2.25 m^3, and an average volumetric error of 46 %. SegmentGS-II (10 to 15 m wide and 5 to 15 m deep gullies) presented total erosion volume of 141.85 m^3 and deposition of 106.03 m^3, and an average volumetric error of 14 %.

DISCUSSION

The volumetric error is the volume of the detection portion that interferes with the uncertainty threshold used in the GCD analysis. High volumetric error values indicate that the spatial and temporal resolution and accuracy of the multi-temporal DEMs series might not be providing adequate sensitivity for GCD analysis.

The detected abrupt changes are due to a mass displacement event that contributed significantly to the increase in erosion and deposition values in this period (Figure 5). In contrast to some studies (Crouch, 1987; Prosser and Slade, 1994), sediment production in the evaluated study area was predominantly composed of mass displacement processes in response to the gradual expansion of the lateral walls of the gully by the formation of the rills. Betts et al. (2003) found similar results.

The differences in volumetric error and altered areas of the segments GS-II, when compared to R and GS-I, can be associated with the fact that segment GS-II presented erosion and deposition events of higher volumetric magnitude in the same period. Thus, the spatial and temporal resolution and the accuracy of the multi-temporal series of DEMs obtained by the methodology of this study were more adequate for the detection of erosion and deposition events of the magnitude presented in this segment in the
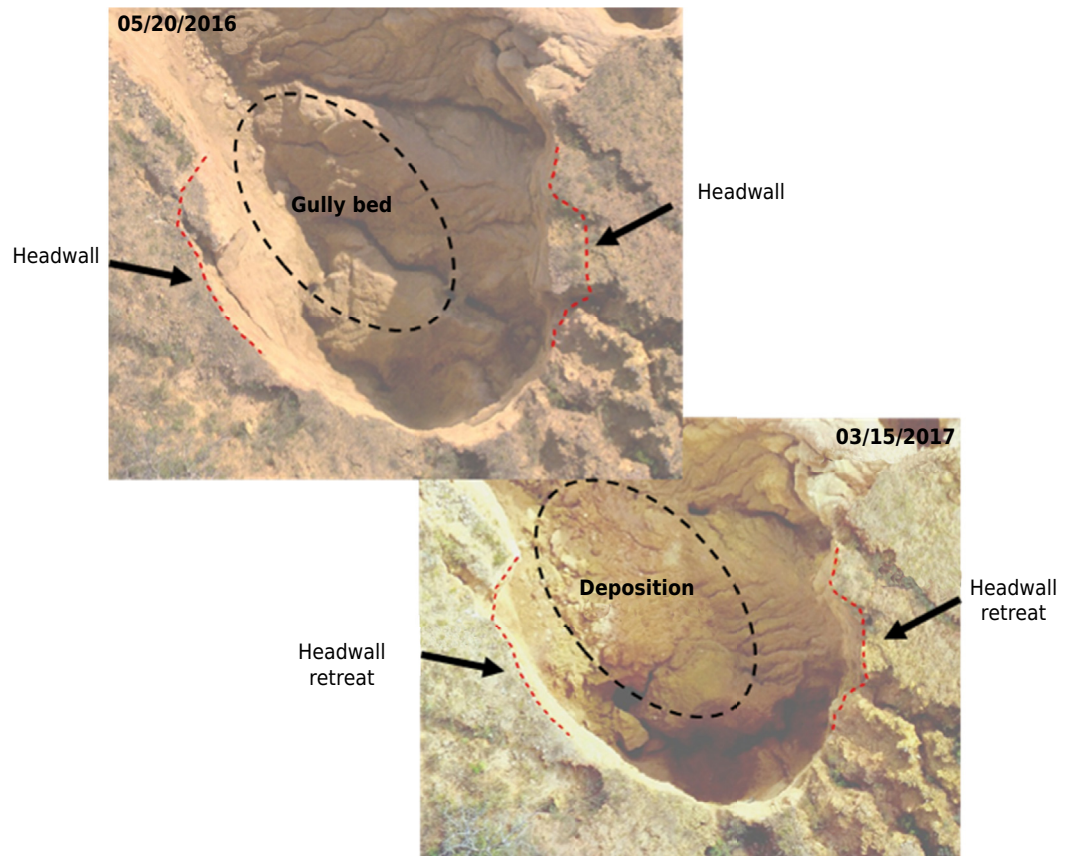
Figure 5. Mass displacement erosion during the studied period between DEM_3 and DEM_1.

studied period. Another aspect is related to the greater dynamics of the erosive process in minor erosion events.

The behaviour observed in figures 4a and 4b was not expected for environments such as rills or small gullies, where it is expected that the evolution of the erosion processes as they suffer the inclement weather of the water erosion provided by the accumulation of rainfall over time (Lin et al., 2015). Such behaviour may be associated to the greater dynamics of the erosive process in smaller erosions, and, since volume of deposition is higher than the eroded volume, probably deposited sediments are originated in the upstream area (De Rose et al., 1998).

The mass displacement processes showed a less clear response to individual events and are more likely to reflect the rains received for longer periods, being influenced by the time required for the water to infiltrate the soil surface, increasing the pressures of the water table to values that are enough to allow the movement of the soil mass (Betts et al., 2003; Vandekerckhove et al., 2003; Hosseinalizadeh et al., 2019). Although small landslides usually occur during or shortly after an erosive event, mass displacements of large magnitude can be considerably delayed as a function of time so that the rainwater infiltrates deep enough to initiate erosive processes (Iverson, 2000).

The methodology used in this study to obtain and analyse the multi-temporal DEMs series was adequate for the monitoring of erosion and soil deposition processes in the GS-II segment, which presented erosion and deposition of the order of 100 m^3 and mean volumetric error of 14 %. By using GCD and orthoimages visual analyses it was possible to detect the events of gully headwall retreat, rill deepening, and sediment deposition (Figure 5), as well as the direct correlation between detected changes and volume rainfall accumulated over time. However, for segments R and GS-I, which presented a percentage of changed area of 2 and 8.6 %, respectively, and erosion and deposition events of the

order of 2 m^3 and volumetric errors of the order of 50 %, the low percentage of detection area and the high percentage of volumetric error indicated that the spatial and temporal resolution and the accuracy of the multi-temporal DEMs series might not be providing adequate sensitivity for GCD analysis applied to erosion monitoring and deposition.

CONCLUSION

The use of multi-temporal series of DEMs obtained by UAV, SfM photogrammetry, and GCD analyses for the monitoring of erosion processes in gullies and rills in the study area was adequate, since it provided quick, low cost, and high resolution orthomorphic digital models of centimetre accuracy. The lower values of volumetric error were associated with higher rates of soil losses, which are the sites that need greater attention in the monitoring and implementation of mitigation measures. For this type of analysis, the adequacy of the spatial and temporal resolution and the accuracy of the DEMs should be considered for the magnitude of the erosion and deposition processes. For gully monitoring studies, the spatial resolution should be at centimetric level, this study obtained 10 and 6 cm for horizontal and vertical resolutions, respectively. Temporal resolution should be according to the rainy seasons, where the largest mass displacements occur.

ACKNOWLEGEMENTS

AUTHOR CONTRIBUTIONS

Conceptualization: Paulo Siqueira Junior (lead) and Marx Leandro Naves Silva (equal).

Methodology: Paulo Siqueira Junior (lead), Bernardo Moreira Candido (equal), Pedro Velloso Gomes Batista (equal), and Wellington de Lima (equal).

Software: Paulo Siqueira Junior (equal) and Bernardo Moreira Candido (equal).

Validation: Paulo Siqueira Junior (lead).

Formal Analysis: Paulo Siqueira Junior (lead), Marx Leandro Naves Silva (equal), Fabio Arnaldo Pomar Avalos (equal), and Pedro Velloso Gomes Batista (equal).

Investigation: Paulo Siqueira Junior (lead), Marx Leandro Naves Silva (lead), Bernardo Moreira Candido (equal), Fabio Arnaldo Pomar Avalos (equal), and Pedro Velloso Gomes Batista (equal).

Resources: Paulo Siqueira Junior (equal), Marx Leandro Naves Silva (lead), and Bernardo Moreira Candido (equal).

Data Curation: Paulo Siqueira Junior (lead), Marx Leandro Naves Silva (equal), Bernardo Moreira Candido (equal), Fabio Arnaldo Pomar Avalos (equal), Pedro Velloso Gomes Batista (equal), and Wellington de Lima (equal).

Writing – Original Draft: Paulo Siqueira Junior (lead), Marx Leandro Naves Silva (equal), Bernardo Moreira Candido (equal), Fabio Arnaldo Pomar Avalos (equal), Pedro Velloso Gomes Batista (equal), and Wellington de Lima (equal).

Writing – review & editing: Marx Leandro Naves Silva (equal), Bernardo Moreira Candido (lead), Fabio Arnaldo Pomar Avalos (equal), Nilton Curi (equal), and John Norman Quinton (equal).

Visualization: Fabio Arnaldo Pomar Avalos (equal).

Supervision: Marx Leandro Naves Silva (lead) and Nilton Curi (equal).

Project Administration: Marx Leandro Naves Silva (lead).

Funding Acquisition: Marx Leandro Naves Silva (lead).

REFERENCES

Betts HD, Trustrum NA, De Rose RC. Geomorphic changes in a complex gully system measured from sequential digital elevation models, and implications for management. Earth Surf Process Landforms. 2003;28:1043-58. https://doi.org/10.1002/esp.500

Casalí J, Loizu J, Campo MA, De Santisteban LM, Álvarez-Mozos J. Accuracy of methods for field assessment of rill and ephemeral gully erosion. Catena. 2006;67:128-38. https://doi.org/10.1016/j.catena.2006.03.005

Castillo C, Pérez R, James MR, Quinton JN, Taguas EV, Gómez JA. Comparing the accuracy of several field methods for measuring gully erosion. Soil Sci Soc Am J. 2012;76:1319-32. https://doi.org/10.2136/sssaj2011.0390

Crouch RJ. The relationship of gully sidewall shape to sediment production. Aust J Soil Res. 1987;25:531-9. https://doi.org/10.1071/SR9870531

Dantas AAA, Carvalho LG, Ferreira E. Classificação e tendências climáticas em Lavras, MG. Cienc Agrotec. 2007;31:1862-6. https://doi.org/10.1590/S1413-70542007000600039

De Rose RC, Gomez B, Marden M, Trustrum NA. Gully erosion in Mangatu Forest, New Zealand, estimated from digital elevation models. Earth Surf Process Landforms. 1998;23:1045-53. https://doi.org/10.1002/(SICI)1096-9837(1998110)23:11<1045::AID-ESP920>3.0.CO;2-T

Di Stefano C, Ferro V, Palmeri V, Pampalone V, Agnello F. Testing the use of an image-based technique to measure gully erosion at Sparacia experimental area. Hydrol Process. 2017;31:573-85. https://doi.org/10.1002/hyp.11048

D'Oleire-Oltmanns S, Marzolff I, Peter KD, Ries JB. Unmanned aerial vehicle (UAV) for monitoring soil erosion in Morocco. Remote Sens. 2012;4:3390-416. https://doi.org/10.3390/rs4113390

Ehiorobo JO, Audu HAP. Monitoring of gully erosion in an urban area using geoinformation technology. J Emerg Trends Eng Appl Sci. 2012;3:270-5.

Gao P. Rill and gully development processes. In: Shroder JF, editor. Treatise on geomorphology. Cambridge: Academic Press; 2013. v. 7. p. 122-31.

Gómez-Gutiérrez A, Schnabel S, De Sanjosé JJ, Contador FL. Exploring the relationships between gully erosion and hydrology in rangelands of SW Spain. Z Geomorphol Supp. 2012;56:27-44. https://doi.org/10.1127/0372-8854/2012/S-00071

Glendell M, McShane G, Farrow L, James MR, Quinton J, Anderson K, Evans M, Benaud P, Rawlins B, Morgan D, Jones L, Kirkham M, DeBell L, Quine TA, Lark M, Rickson J, Brazier RE. Testing the utility of structure-from-motion photogrammetry reconstructions using small unmanned aerial vehicles and ground photography to estimate the extent of upland soil erosion. Earth Surf Process Landforms. 2017;42:1860-71. https://doi.org/10.1002/esp.4142

Hosseinalizadeh M, Kariminejad N, Chen W, Pourghasemi HR, Alinejad M, Behbahani AM, Tiefenbacher JP. Spatial modelling of gully headcuts using UAV data and four best-first decision classifier ensembles (BFTree, Bag-BFTree, RS-BFTree, and RF-BFTree). Geomorphology. 2019;329:184-93. https://doi.org/10.1016/j.geomorph.2019.01.006

Iverson RM. Landslide triggering by rain infiltration. Water Resour Res. 2000;36:1897-910. https://doi.org/10.1029/2000WR900090

IUSS Working Group WRB. World reference base for soil resources 2014, update 2015: International soil classification system for naming soils and creating legends for soil maps. Rome: Food and Agriculture Organization of the United Nations; 2015. (World Soil Resources Reports, 106).

Lin J, Huang Y, Wang M-k, Jiang F, Zhang X, Ge H. Assessing the sources of sediment transported in gully systems using a fingerprinting approach: an example from South-east China. Catena. 2015;129:9-17. https://doi.org/10.1016/j.catena.2015.02.012

Ouédraogo MM, Degré A, Debouche C, Lisein J. The evaluation of unmanned aerial system-based photogrammetry and terrestrial laser scanning to generate DEMs of agricultural watersheds. Geomorphology. 2014;214:339-55. https://doi.org/10.1016/j.geomorph.2014.02.016

Passalacqua P, Belmont P, Staley DM, Simley JD, Arrowsmith JR, Bode CA, Crosby C, DeLong SB, Glenn NF, Kelly SA, Lague D, Sangireddy H, Schaffrath K, Tarboton DG, Wasklewicz T, Wheaton JM. Analyzing high resolution topography for advancing the understanding of mass and energy transfer through landscapes: a review. Earth-Sci Rev. 2015;148:174-93. https://doi.org/10.1016/j.earscirev.2015.05.012

Poesen J, Nachtergaele J, Verstraeten G, Valentin C. Gully erosion and environmental change: importance and research needs gully erosion and environmental change. Catena. 2003;50:91-133. https://doi.org/10.1016/S0341-8162(02)00143-1

Prosser IP, Slade CJ. Gully formation and the role of valley-floor vegetation, southeastern Australia. Geology. 1994;22:1127-30. https://doi.org/10.1130/0091-7613(1994)022<1127:GFAT RO>2.3.CO;2

Santos HG, Jacomine PKT, Anjos LHC, Oliveira VA, Lumbreras JF, Coelho MR, Almeida JA, Araújo Filho JC, Oliveira JB, Cunha TJF. Sistema brasileiro de classificação de solos. 5. ed. rev. ampl. [e-book]. Brasília, DF: Embrapa; 2018.

Soil Survey Staff. Keys to soil taxonomy. 12th ed. Washington, DC: United States Department of Agriculture, Natural Resources Conservation Service; 2014.

Stöcker C, Eltner A, Karrasch P. Measuring gullies by synergetic application of UAV and close range photogrammetry - a case study from Andalusia, Spain. Catena. 2015;132:1-11. https://doi.org/10.1016/j.catena.2015.04.004

Tarolli P. High-resolution topography for understanding Earth surface processes: opportunities and challenges. Geomorphology. 2014;216:295-312. https://doi.org/10.1016/j.geomorph.2014.03.008

Vandekerckhove L, Poesen J, Govers G. Medium-term gully headcut retreat rates in Southeast Spain determined from aerial photographs and ground measurements. Catena. 2003;50:329-52. https://doi.org/10.1016/S0341-8162(02)00132-7

Wang R, Zhang S, Pu L, Yang J, Yang C, Chen J, Guan C, Wang Q, Chen D, Fu B, Sang X. Gully erosion mapping and monitoring at multiple scales based on multi-source remote sensing data of the Sancha River Catchment, Northeast China. ISPRS Int J Geo-Inf. 2016;5:200-16. https://doi.org/10.3390/ijgi5110200

Wheaton JM, Brasington J, Darby SE, Sear DA. Accounting for uncertainty in DEMs from repeat topographic surveys: improved sediment budgets. Earth Surf Process Landforms. 2010;35:136-56. https://doi.org/10.1002/esp.1886